Research on Lithium Niobate-based Photonic Crystal with Wide Bandgap

Dingwei Chen, Jiangbo Wu, Xiang Zheng, Xing Yan, Changjin Hu, Jian Li, Yongjun Huang, and Guangjun Wen

School of Information and Communication Engineering
Sichuan Provincial Engineering Research Center of Communication Technology for Intelligent IoT
University of Electronic Science and Technology of China, Chengdu 611731, China

2022 Photonics & Electromagnetics Research Symposium (PIERS) | 978-1-6654-6023-1/22/$31.00 ©2022 IEEE | DOI: 10.1109/PIERS55526.2022.9793145

Abstract— Photonic crystal is a structure formed by arranging materials with different dielectric coefficients in space according to a certain period. Photonic crystal has a variety of applications, e.g., can be used to design photonic crystal fibers, cavity optomechanics, photonic crystal antennas, etc. Most of the raw materials for the photonic crystal are Si, SiN, GaAs, etc., and lithium niobate is a new type of photonic crystal material, because of its rich photoelectric effect, stable physical and chemical properties, and wide light transmission range. With the continuous development of lithium niobate single crystal thin film processing technology, it is now possible to provide single crystal thin film lithium niobate with a thickness of 300–900 nm, making it possible to use lithium niobate for photonic crystal fabrications. Therefore, this paper investigates and simulates the wide bandgap characteristics of lithium niobate photonic crystals. By using finite difference time domain (FDTD) method, the simulations and investigations of the photonic bandgap in a hole-shaped lithium niobate on insulator silica is provided in this paper, through controlling the ratio among the lattice constant, the radius of the air hole layer and the thickness of lithium niobate layer. The results indicate that the radius of the air hole and the thickness of the lithium niobate photonic crystal will affect the center wavelength and bandwidth of the photonic crystal bandgap. And when the ratio of the radius to the lattice constant is about 0.35, by adjusting the thickness of the lithium niobate, a lithium niobate photonic crystal with a wide bandgap of 1387 nm–1726 nm is obtained. Based on this optimization results, the lithium niobate photonic crystal cavity with high Q factor, and also the lithium niobate photonic crystal optomechanical cavity can be achieved.

1. INTRODUCTION

Photonic crystals (PhC) have the ability to control the movement of light in photonic crystals through their optical band gap. Based on this ability, a variety of new photonic devices based on photonic crystals have been proposed one after another, including thresholdless lasers [1], lossless mirrors and bending Optical path [2], optical microcavity with high quality factor [3–6], nonlinear switch [7] and amplifier with low drive energy, super prism [8] with extremely high wavelength resolution and small size, photonic crystal fiber [9] with dispersion compensation, and light-emitting diode with improved efficiency. The emergence of photonic crystals makes it possible to "full photonization" of information processing technology and the miniaturization and integration of photonic technology. It may lead to a revolution in information technology in the future, and its impact may be comparable to that of semiconductor technology in the past. The two-dimensional photonic crystal slab has significant advantages in many photonic crystal structures, including low processing difficulty, flexible structure design, and the scalability of optoelectronic integration. These advantages make 2D photonic crystal slabs developed based on various material platforms have been continuously proposed.

Lithium niobate (LN), due to its excellent material properties (rich photoelectric effect, stable physical and chemical properties, wide light transmission range, low optical loss), has a wide range of applications in the optical field, and is called photonic silicon. New designs of 2D photonic crystals based on the lithium niobate material platform are also constantly being proposed. Many applications of photonic crystals are based on the existence and size of photonic band gaps. The wider the band gap, the wider the frequency of prohibiting light from spreading, and the larger the range of applications. Therefore, the design of photonic crystals with large band gap width is an important part of the study of PhC materials.

Herein, we use the FDTD method, considering the dispersion of the LN and the thickness of the slab to accurately simulate the band gap structure of the LN PhC slab, and propose a wide band gap LN PHC Slab with a band gap range of 1387–1726 nm. Through systematic simulation of the PHC slab band gap structure under different lattice constants, different radius-lattice constant ratios,

and different thickness-lattice constant ratios, the relationship between the structural parameters of the LN PHC slab and the band gap structure is obtained.

2. CALCULATION METHOD AND THEORY OF PHOTONIC CRYSTAL BAND GAP STRUCTURE

2.1. Maxwell's Equations in Photonic Crystals

The theoretical research problem of photonic crystals can be attributed to the problem of light propagation in photonic crystals, so it can be solved by the macroscopic Maxwell equations. The Maxwell equations of photonic crystals described as following:

$$\nabla \times \mathbf{H} = \varepsilon(r) \frac{\partial \mathbf{E}}{\partial t} \tag{1}$$

$$\nabla \times \mathbf{E} = -\mu_0 \frac{\partial \mathbf{H}}{\partial t} \tag{2}$$

In the formula, **H** and**E** are the magnetic field intensity and electric field intensity of the light wave in the photonic crystal, μ_0 is the vacuum permeability, and $\varepsilon(r)$ is the dielectric constant of the photonic crystal, which is a function of space coordinates; theories about photonic crystals The focus of the calculation is how to solve the above Maxwell equations from the distribution of the known dielectric constant ε.

2.2. Finite Difference Time Domain Method

The finite difference time domain (FDTD) method uses the difference of space and time instead of differentiation, adopts the two-dimensional finite difference time domain method proposed by YEE to grid the photonic crystal unit [10] (E polarization distribution is shown in the Figure 1. Use Δx, Δy to denote the spatial step length in the x and y directions, and Δt to denote the time step).

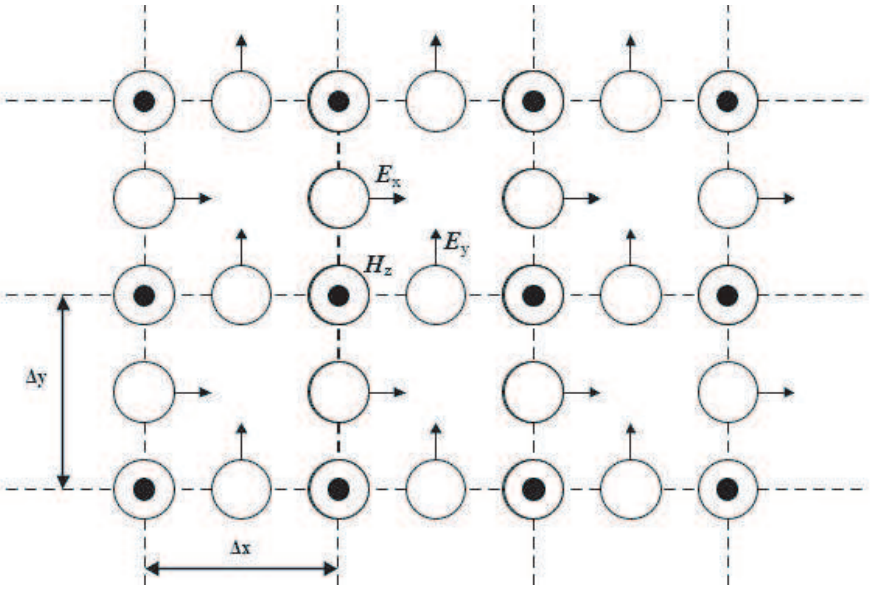

Figure 1: Yee's 2-D differential lattice.

Using the central difference instead of the differential in Equation (1), Maxwell's equation can

be transformed into an iterative form of FDTD equation:

$$\begin{aligned}\mathbf{H}_z^{n+1/2}(i+1/2,j+1/2) &= \mathbf{H}_z^{n-1/2}(i+1/2,j+1/2)+\frac{\Delta t}{\mu(i+1/2,j+1/2)\Delta y}\\ &\cdot\left[\mathbf{E}_x^n(i+1/2,j+1)-\mathbf{E}_x^n(i+1/2,j)\right]-\frac{\Delta t}{\mu(i+1/2,j+1/2)\Delta x}\\ &\times\left[\mathbf{E}_y^n(i,j+1/2)-\mathbf{E}_y^n(i+1,j+1/2)\right] \quad (3)\\ \mathbf{E}_x^{n+1}(i+1/2,j) &= \mathbf{E}_x^n(i+1/2,j)+\frac{\Delta t}{\varepsilon(i+1/2,j)\Delta y}\\ &\left[\mathbf{H}_z^{n+1/2}(i+1/2,j+1/2)-\mathbf{H}_Z^{n+1/2}(i+1/2,j-1/2)\right] \quad (4)\\ \mathbf{E}_y^{n+1}(i,j+1/2) &= \mathbf{E}_y^n(i,j+1/2)+\frac{\Delta t}{\varepsilon(i,j+1/2)\Delta x}\\ &\left[\mathbf{H}_z^{n+1/2}(i-1/2,j+1/2)-\mathbf{H}_Z^{n+1/2}(i+1/2,j+1/2)\right] \quad (5)\end{aligned}$$

In the formula, i and j are the node numbers in the x and y directions in the grid respectively. Similar calculation formulas for H_x, H_y and E_z can also be obtained for the TM mode. The time evolution law of the electromagnetic field can be obtained according to the discrete FDTD time discrete step formula (3), (4) and (5). In order to ensure that iterative convergence obtains a stable solution, the selection of Δx, Δy, and Δt must satisfy the Courant condition [11]:

$$c\Delta t=\frac{1}{\sqrt{\frac{1}{\Delta x^2}+\frac{1}{\Delta y^2}}} \quad (6)$$

When using the FDTD method to study the transmission characteristics of photonic crystals, the calculation area is limited, that is, the space occupied by the volume of the photonic crystal. Due to the limited computer processing power, the number of grids that can be calculated is limited. In order to simulate the electromagnetic scattering process with higher accuracy after considering the material dispersion and structure thickness, the simulation area can be reduced and the perfect matching layer can be introduced.

From the above formula, we can calculate the electric and magnetic field alternately sampling according to formulas (1)–(6) by given the initial value of the electromagnetic field distribution and the refractive index distribution everywhere, and obtain the value of each component of the space electromagnetic field at each time.

2.3. Finite Difference Time Domain Method

In the simulation model, in order to reduce the calculation requirements of the model, 5 columns are taken in the y direction and 4 rows are taken in the x direction. In the calculation, the dielectric constant of the air hole is 1.0, the periodic boundary conditions are used in the x and y directions, and the PML boundary conditions are used in the z direction. Use **a**, **r**, and **z** to denote the lattice constant, the radius of the air hole and the thickness of the slab, respectively. Three types of models are introduced. The first model A does not consider dispersion. According to the working wavelength of 1550nm, the ordinary refractive index and the extraordinary refractive index of the ln material are set to $\mathbf{n_0} = 2.21509$ and $\mathbf{n_e} = 2.14101$. The second model B does not consider the thickness and sets the thickness z to infinite. The third model C considers both thickness and dispersion.as a result,the simulation results will be closer to reality. LN has birefringence characteristics, and its refractive index is given in the form of sellmeier equation:

$$n_o^2 = 4.9048-\frac{0.11768}{0.04750-\lambda^2}-0.027169\lambda^2 \quad (7)$$

$$n_e^2 = 4.5820-\frac{0.099169}{0.044432-\lambda^2}-0.021950\lambda^2 \quad (8)$$

3. RESULTS AND DISCUSSION

3.1. Influence of Dispersion and Thickness on the Simulation Results of Band Gap Structure

When using the FDTD method to analyze and calculate the energy band structure of the LN PHC, due to the large amount of calculation, ignoring the thickness and dispersion has become

a common way to reduce the difficulty of calculation. In this section, we introduce the fixed structure parameters into the three types of models in Section 2.3 for simulation, and obtain the influence of dispersion and thickness on the simulation results of the band gap structure. We take the structure ratio of a specific wide band gap LN PhC Slab as an example, in this example $\mathbf{a} : \mathbf{r} : \mathbf{z} = 1 : 0.35 : 0.8$. The simulation results of the three types of models are shown in the following table (Table 1):

Table 1: Physical parameters.

Name	Normalized band gap width	Normalized band gap center
A	0.0611	0.427
B	0.0528	0.381
C	0.0934	0.429

As shown in Table 1, the band gap center position of model A without considering dispersion is basically the same as the band gap center position of model C, but the band gap width of model A is significantly smaller than model C, with an error of about 30%. Model B, which does not consider the thickness, has a large deviation between the center of the band gap and the width of the band gap, and its band gap width is significantly smaller than that of Model C. Therefore, in order to determine the center position of the band gap, we can use a model that does not consider dispersion to reduce the calculation requirements. In order to obtain accurate band gap simulation results, study the relationship between the band gap and structural parameters and find the wide band gap LN PHC slab, a model that considers dispersion and thickness at the same time is a reasonable choice.

3.2. Influence of Structural Parameters on the Position and Width of the Band Gap

First, we study the influence of the lattice constant **a** on the position and width of the band gap of the LN PHC slab. By keeping the ratio of $\mathbf{a} : \mathbf{r} : \mathbf{z}$ unchanged in model C and changing the value of **a** for simulation, we get the result shown in Figures 2(a) and (b). It can be found that under the condition of three ratios of $\mathbf{a} : \mathbf{r} : \mathbf{z}$, the crystal lattice constant **a** has no significant effect on the normalized band gap width and the normalized band gap average. The working wavelength of the photonic crystal can be calculated by dividing the lattice constant a by the normalized frequency, so the lattice constant **a** can be used to determine the operating wavelength of LN PHC slab.

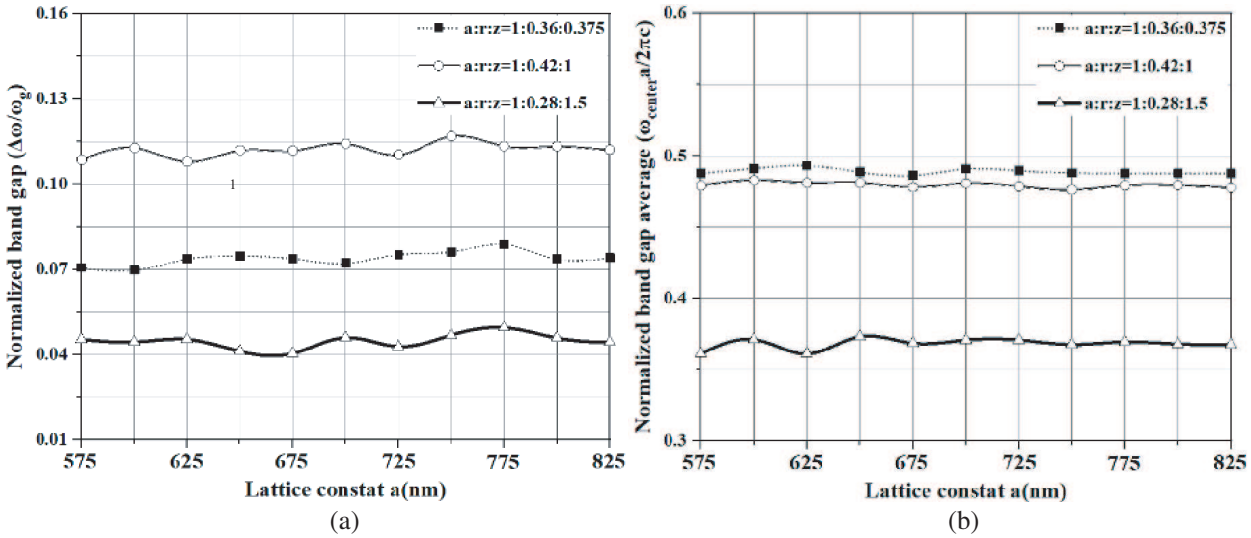

Figure 2: (a) Normalized band gap under different lattice constants and parameter ratios; (b) Normalized band gap under different lattice constants and parameter ratios.

Secondly, we study the influence of the air hole radius **r** on the position and width of the LN PHC slab band gap. In model C, we simulated the photonic crystal plate under three different $\mathbf{z}/\mathbf{a}$ ratio conditions ($\mathbf{z}/\mathbf{a} = 0.5, 0.625, 0.7$) with $\mathbf{r}/\mathbf{a}$ as the independent variable. The relationship between $\mathbf{r}/\mathbf{a}$ and band gap width is shown in Figure 3(a). It can be seen that when $\mathbf{r}/\mathbf{a}$ is in the range of

0.325 to 0.425, the change of band gap width tends to be stable, and there is a maximum band gap width. Value. When r/a exceeds this range, the band gap width will be significantly reduced. The relationship between r/a and the position of the band gap center is shown in Figure 3(b). According to the data, when $\mathbf{z/a}$ is determined, the normalized band gap average will increase with the increase of $\mathbf{r/a}$, that is, the working wavelength will decrease as $\mathbf{r/a}$ increases.

After that, we study the influence of thickness $\mathbf{z}$ on the position and width of the band gap of the LN PHC slab. In the same way as the research of $\mathbf{r/a}$, we kept $\mathbf{r/a}$ unchanged, and performed simulations with $\mathbf{z/a}$ as the independent variable under three different $\mathbf{r/a}$ ratio conditions. The relationship between $\mathbf{z/a}$ and the band gap width is shown in Figure 4(a). It can be found that as $\mathbf{z/a}$ increases, the band gap width first increases, then tends to stabilize, and finally decreases rapidly. And the larger the value of r/a, the larger the value of z/a when the band gap width begins to decrease significantly. When $\mathbf{r} = 0.28\mathbf{a}$, $0.35\mathbf{a}$ and $0.42\mathbf{a}$, the band gap width starts to decrease from $\mathbf{z/a} = 1.65$, $\mathbf{z/a} = 1.5$ and $\mathbf{z/a} = 1.25$. The relationship between z/a and the position of the band gap center is shown in Figure 4(b). From this figure, it can be known that when r/a is determined, the normalized band gap average value will decrease with the increase of r/a, that is, working The wavelength will increase as $\mathbf{z/a}$ increases.

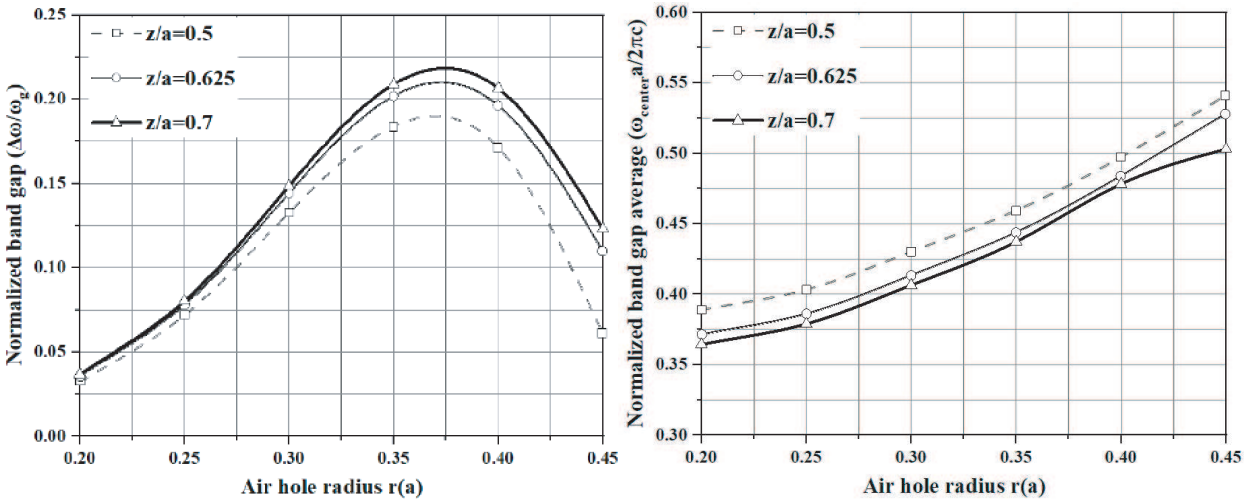

(a) (b)

Figure 3: (a) Normalized band gap under three kinds of $\mathbf{z/a}$ conditions with different $\mathbf{r/a}$; (b) Normalized band gap under three kinds of $\mathbf{z/a}$ conditions with different $\mathbf{r/a}$.

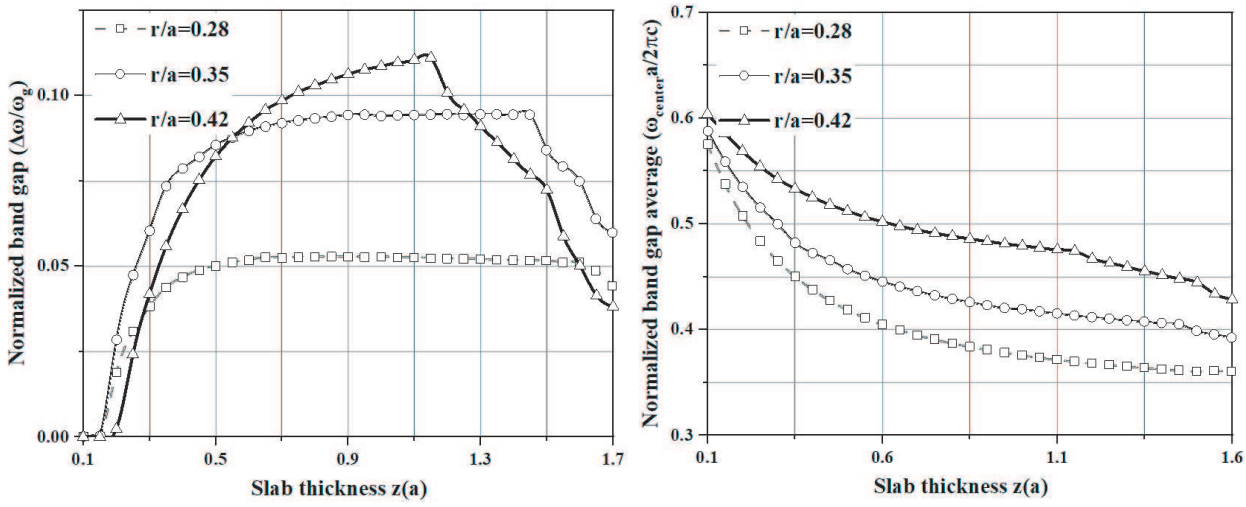

(a) (b)

Figure 4: (a) Normalized band gap under three kinds of $\mathbf{r/a}$ conditions with different $\mathbf{z/a}$; (b) Normalized band gap under three kinds of $\mathbf{r/a}$ conditions with different $\mathbf{z/a}$.

Finally, after determining the influence of the LN PhC slab structure parameters on the position and width of the band gap, we found a wide band gap LN PhC slab structure that works near 1550 nm, with $\mathbf{a} = 660$ nm, $\mathbf{r} = 231$ nm, $\mathbf{z} = 528$ nm, and its prohibition band range is between $\omega\mathbf{a}/\mathbf{2}\pi\mathbf{c} = 0.382303$ and $\omega\mathbf{a}/\mathbf{2}\pi\mathbf{c} = 0.475712$. The corresponding wavelength range is 1387–1726 nm, and the band gap is 336 nm. The energy band structure is shown in Figure 5.

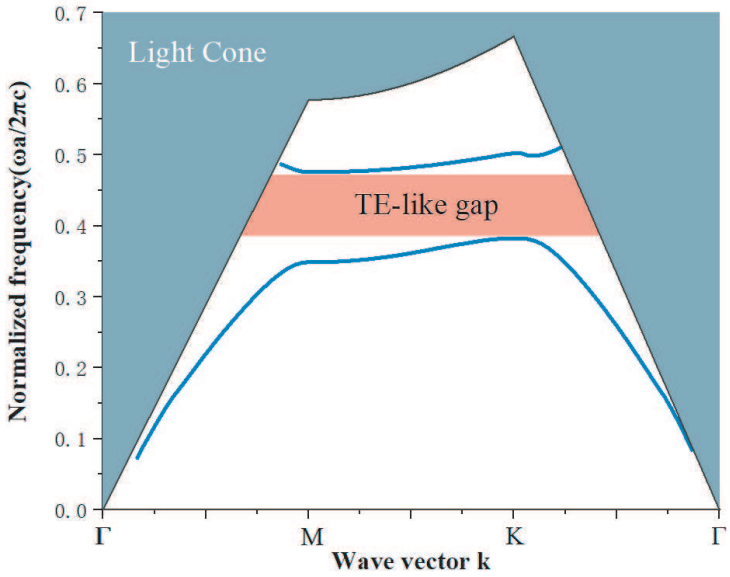

Figure 5: Band structure of wide band gap LN PhC slab.

4. CONCLUSION

In conclusion, this paper establishes an FDTD simulation model that considers both the dispersion of the lithium niobate material and the thickness of the LN PHC slab to study the influence of the dispersion and thickness parameters on the band gap simulation results. The relationship between the structural parameters and the band gap of LN PhC Slab is systematically analyzed. A systematic analysis of the relationship was carried out. Based on the results, a LN PhC slab with a band gap of 336 nm and working at 1550 nm has been designed.

ACKNOWLEDGMENT

This work was supported in part by the National Natural Science Foundation of China under project contracts No. 61971113 and No. 61901095, in part by National Key R&D Program under project contract No. 2018YFB1802102 and No. 2018AAA0103203, in part by Guangdong Provincial Research and Development Plan in Key Areas under project contract No. 2019B010141001 and No. 2019B010142001, in part by Sichuan Provincial Science and Technology Planning Program of China under project contracts No. 2020YFG0039, No. 2021YFG0013, and No. 2021YFH0133, in part by the fundamental research funds for the Central Universities under project contract No. ZYGX2019Z022, in part by the Yibin Science and Technology Planning Program under project contracts No. 2018ZSF001 and No. 2019GY001, in part by the Ministry of Education-China Mobile Research Fund under project contracts No. MCM20180104, in part by Intelligent Terminal Key Laboratory of Sichuan Province under project contract No. SCITLAB-0010, and in part by the Guangxi Key Laboratory of Wireless Wideband Communication and Signal Processing under project contract No. GXKL06200209.

REFERENCES

1. Shi, L.-T., F. Jin, M.-L. Zheng, X.-Z. Dong, W.-Q. Chen, Z.-S. Zhao, and X.-M. Duan, "Low threshold photonic crystal laser based on a rhodamine dye doped high gain polymer," *Physical Chemistry Chemical Physics: PCCP*, Vol. 18, No. 7, 5306–5315, 2016.
2. Beravat, R., G. K. L. Wong, M. H. Frosz, X. M. Xi, and P. St. J. Russell, "Twist-induced guidance in coreless photonic crystal fiber: A helical channel for light," *Science Advances*, Vol. 2, No. 11, e1601421–e1601421, 2016.

3. Li, M., H. Liang, R. Luo, Y. He, and Q. Lin, "High-Q 2D Lithium Niobate photonic crystal slab nanoresonators," *Laser & Photonics Reviews*, Vol. 13, No. 5, 1800228-N/a, 2019.
4. Li, M., H. Liang, R. Luo, Y. He, J. Ling, and Q. Lin, "Photon-level tuning of photonic nanocavities," *Optica*, Vol. 6, No. 7, 860, 2019.
5. Liang, H., R. Luo, Y. He, H. Jiang, and Q. Lin, "High-quality Lithium Niobate photonic crystal nanocavities," *Optica*, Vol. 4, No. 10, 1251, 2017.
6. Jiang, W., R. N. Patel, F. M. Mayor, T. P. McKenna, P. Arrangoiz-Arriola, C. J. Sarabalis, J. D. Witmer, R. Van Laer, and A. H. Safavi-Naeini, "Lithium Niobate Piezo-optomechanical crystals," *Optica*, Vol. 6, No. 7, 845, 2019.
7. Wirth Lima, A. and A. S. B. Sombra, "Graphene-photonic crystal switch," *Optics Communications*, Vol. 321, 150–156, 2014.
8. Jugessur, A., L. Wu, A. Bakhtazad, A. Kirk, T. Krauss, and R. De La Rue, "Compact and integrated 2-D photonic crystal super-prism filter-device for wavelength demultiplexing applications," *Optics Express.*, Vol. 14, No. 7, 1632–1642, 2006.
9. Zhao, Y., F. Xia, H.-F. Hu, and M.-Q. Chen, "A novel photonic crystal fiber Mach-Zehnder interferometer for enhancing refractive index measurement sensitivity," *Optics Communications*, Vol. 402, 368–374, 2017.
10. Yee, K., "Numerical solution of initial boundary value problems involving Maxwell's Equations in isotropic media," *IEEE Transactions on Antennas and Propagation*, Vol. 14, No. 3, 302–307, 1966.
11. Oskooi, A. F., D. Roundy, M. Ibanescu, P. Bermel, J. D. Joannopoulos, and S. G. Johnson, "Meep: A flexible free-software package for electromagnetic simulations by the FDTD method," *Computer Physics Communications*, Vol. 181, No. 3, 68–702, 2010.